Fluctuations in the homeostatic neural circuitry influence consistency in choices between cultural goods

Azzalini D.*, Buot A., Palminteri S. & Tallon-Baudry C.*

Laboratoire de Neurosciences Cognitives et Computationnelles, Ecole Normale Supérieure, PSL University & Institut National de la Santé et de la Recherche Médicale, Paris, France

* Corresponding authors (damiano.azzalini@ens.fr, catherine.tallon-baudry@ens.fr)

Keywords

Decision-making, preferences, heartbeat-evoked response, MEG, value-based decision, visceral signals, subjectivity

Summary

Preferences for primary goods, such as food items, are variable and depend on current physiological state. Decisions on cultural goods, entailing no direct physiological consequence, rely on the same neural underpinnings of valuation and choice than primary goods. Here, we test whether subjective preferences for cultural goods inherit a functional link with the neural circuitry monitoring physiological variables. Using magnetoencephalography in human participants choosing between two movies, we measured heartbeat-evoked responses (HERs), which index the cortical monitoring of cardiac contractions. Trial-by-trial fluctuations in HERs, measured before option presentation, influenced the subsequent neural encoding of subjective value in ventro-medial prefrontal cortex - a region involved both in valuation and cardiac monitoring. The neural interaction between HERs and value encoding enhanced trial-by-trial choice precision and predicted inter-individual differences in choice consistency. The enhanced monitoring of physiological variables thus supports more stable representations of subjective, self-related cognitive information.

Introduction

Do you prefer a handful of potato chips or a slice of cake? Forrest Gump or Matrix? Both kinds of choice rely on the estimation of the subjective value of each option and their comparison, a process that engages in particular ventro-medial prefrontal cortex (vmPFC) (Chib et al., 2009; Lebreton et al., 2009; Levy and Glimcher, 2011; McNamee et al., 2013; Sescousse et al., 2013). The primary goal of dietary choices is to restore potential homeostatic imbalance of the organism. In this view, option values are determined by the distance between the current state of the organism and an homeostatic set-point (Juechems and Summerfield, 2019; Keramati and Gutkin, 2014).To achieve this, several physiological parameters (Abitbol et al., 2015; McNamara et al., 2012) indexing the current state of the organism are integrated in the evaluation process. For example, choosing crisps over cake is more valuable because if it helps compensate a low salt blood level, while cake would be preferred in another metabolic context (Berthoud, 2011; Loewenstein, 1996; Rangel, 2013; Small et al., 2001). Because of their importance for survival and evolutionary ancient origin, choices between primary goods such as food items have shaped decisional neural mechanisms. Choices between cultural goods such as movies entail no immediate physiological consequences, but rely on the same cortical valuation network employed for primary goods (Chib et al., 2009; Lebreton et al., 2009; Levy and Glimcher, 2011; McNamee et al., 2013; Sescousse et al., 2013). Choices between secondary goods are thus likely to have inherited a tight link with the neural circuitry involved in homeostatic regulation.

This inheritance generates two opposite predictions. On the one hand, the neural representation of physiological variables when choosing between cultural

items is task-irrelevant and introduces noise. In this view, the integration of physiological variables would be detrimental to the stability of decisions (Loewenstein, 1996), and may account for part of the "neural noise" of mostly unknown origin that would account for variability in preference-based decision-making (Fehr and Rangel, 2011; Padoa-Schioppa, 2013). Alternatively, the neural read-out of physiological variables might improve preference-based decisions, even for cultural goods, by providing a more reliable self-representation of the decision-maker. Indeed, preference-based decisions are intrinsically subjective and require individuals to reflect upon themselves to determine the subjective values of the available options.

A long tradition associates physiological and bodily signals with different aspects of selfhood (Azzalini et al., 2019; Blanke et al., 2015; Damasio, 2010; Park and Tallon-baudry, 2014). Among the numerous physiological signals monitored by the brain, heartbeats have a special status. Heartbeats act as internal stimuli that are constantly and automatically monitored, generating a transient neural response at each heartbeat, also known as the heartbeat evoked response (HER) (Azzalini et al., 2019; Park and Tallon-baudry, 2014; Schandry et al., 1986). HERs have also been shown to correlate with subjective and self-related cognitive content in vmPFC (Babo-Rebelo et al., 2016b, 2016a). Therefore, the neural monitoring of heartbeats in vmPFC might improve the consistency of preference-based choices because it improves the reliability of internal, subjective evidence.

To test these two alternative accounts, we asked participants to perform either a subjective, preference-based choice, as well as a control, objective

perceptual discrimination, between two visually presented movie titles (**Fig. 1A**), while their neural and cardiac activity were measured with magnetoencephalograhy (MEG) and electrocardiography (ECG), respectively. Each trial began with a symbol instructing participants which type of decision to perform. In subjective preference trials, participants selected the movie they preferred, while in the objective perceptual discrimination trials they had to indicate the movie title written with the highest contrast. We measured HERs during the instruction period, tested how they influenced the neural representation of value (**Fig. 1B**), and determined whether this influence improved, or decreased, choice consistency with respect to likeability ratings obtained the day before the recording session (**Supplementary Fig. 1**).

Results

Behavioral results

Participants were asked to choose between two simultaneously presented movie titles according either to their subjective preferences or to the visual contrast of movie titles, as indicated by trial-by-trial instructions presented before the alternatives (**Fig. 1A**). Decision difficulty, operationalized as the difference between the two options (difference between likeability ratings measured one day before the MEG session in the preference task, difference between contrasts in the perceptual task), had the expected impact on behavior in both tasks. Accuracy increased and reaction times decreased for easier decisions (**Fig. 1C**; preference task: one-way repeated measures ANOVA, main effect of difficulty, accuracy, $F_{(3,60)} = 99.25$, $p < 10^{-15}$; RT, $F_{(3,60)} = 41.14$, $p < 10^{-13}$; perceptual task: main effect of difficulty, accuracy, $F_{(3,60)} = 280.2$, $p < 10^{-15}$; RT, $F_{(3,60)} = 87.67$, $p < 10^{-15}$). Preference and perceptual decisions were matched in accuracy (two-way repeated measures ANOVA, main effect of task on accuracy, $F_{(1,20)} = 0.38$, $p = 0.55$, interaction between task and difficulty, $F_{(3,60)} = 2.53$, $p = 0.07$). However, preference-based decisions were generally slower (two-way repeated measures ANOVA, main effect of task, RT, $F_{(1,20)} = 57.64$, $p < 10^{-6}$) and reaction times decreased less rapidly for easier decisions (interaction effect between task and difficulty, $F_{(3,60)} = 4.08$, $p = 0.01$). Although the stimuli were identical in the two tasks, participants only used task-relevant information (subjective value or contrast) to reach their decision, since non-relevant information could not predict choice (**Fig. 1D**; **Supplementary Table 1**).

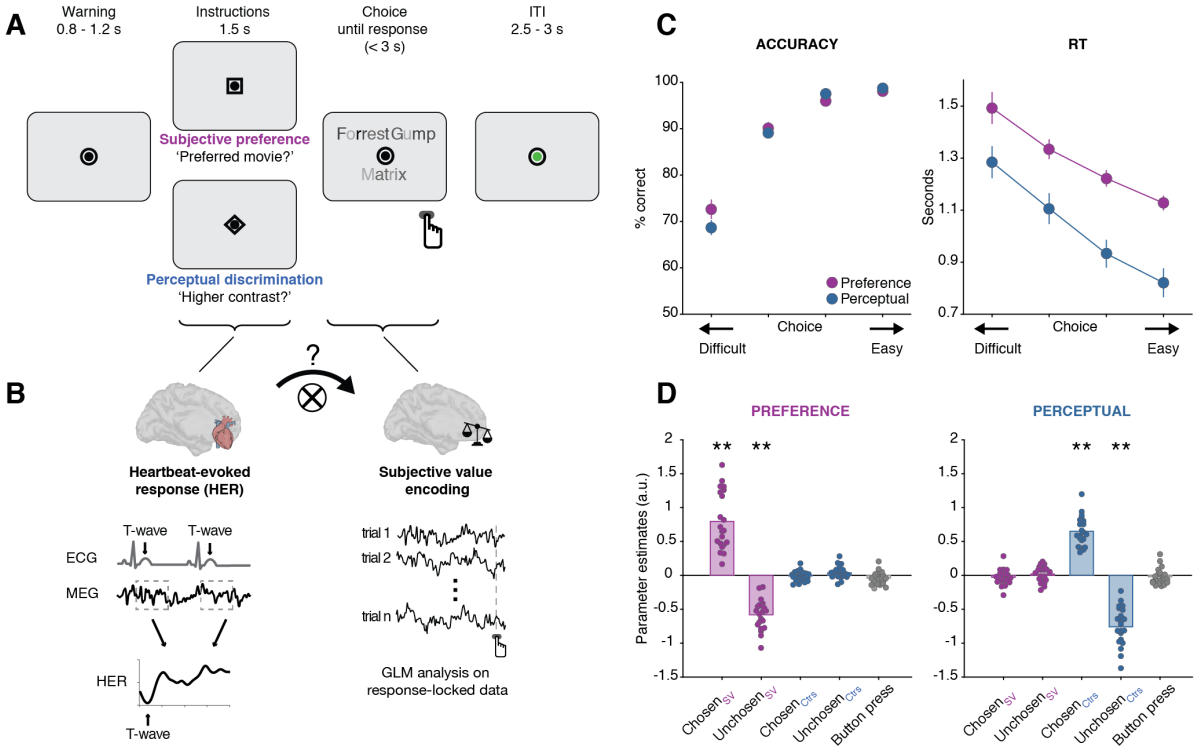

Fig. 1. Experimental design and behavioral results. **A**, Trial time-course. Each trial started with a fixation period of variable duration. The subsequent square or a diamond symbol instructed participants about the type of decision they had to perform on the upcoming movie titles, a subjective preference-based choice or an objective perceptual discrimination task. Decision type varied on a trial-by-trial basis. The two movie titles then appeared above and below fixation and remained on screen until response or until 3 seconds had elapsed. **B**, Rationale for data analysis. Left, heartbeat-evoked responses (HERs) were computed during the instruction period, before option presentation, by locking MEG activity to the T-waves of the electrocardiogram. Right, response-locked MEG activity during choice was modeled on a trial-by-trial basis with a GLM to isolate the spatio-temporal patterns of neural activity encoding value. The central question is whether HERs and value encoding interact. **C**, Behavioral results. In both tasks accuracy increased ($F(3,60) = 99.25$, $p < 10^{-15}$) and response times decreased ($F(3,60) = 41.14$, $p < 10^{-13}$) for easier choices (i.e. larger difference in subjective value for preference-based decisions, or difference in contrast for perceptual ones). **D**, Only task-relevant information significantly contributed to choice in both preference-based and perceptual decisions as estimated by logistic regression (two-tailed t-test against zero). **p<0.01.

Neural responses to heartbeats are larger when preparing for preference-based decisions

Because preference-based choices are intrinsically subjective, we hypothesized that HERs would be larger when preparing for subjective, preference-based decisions than when preparing for objective, perceptual ones, during the instruction period, before the options were presented. We found that HERs during the instruction period were larger when participants prepared for preference-based decisions than for perceptual ones (**Fig. 2A**, **2B**; non-parametric clustering, 201-262 ms after T-wave, sum(t) = 1789, Monte Carlo cluster level p = 0.037). The cortical regions that mostly contributed to this effect (**Fig. 2C**, **Table 1**) were localized in right and left anterior vmPFC (corresponding to areas 11m and 14, bilaterally; cluster peak at MNI coordinates, right [1 57 -21] left [-3 47 -6]), in the right post-central complex ([32 -22 56]) and right supramarginal gyrus ([41 -33 43]).

The HER difference between subjective, preference-based trials and objective, perceptual discrimination trials was not accompanied by any difference in ECG activity (**Supplementary Table 2**), in cardiac parameters (inter-beat intervals, inter-beat intervals variability, stroke volume) or arousal indices (alpha power and pupil diameter) measured during the instruction period (**Supplementary Table 3**). In addition, the difference was locked to heartbeats and was not due to shifts in baseline activity between conditions (Monte-Carlo p=0.026. see **Methods** for details).

The subjective value of the chosen option during preference decisions is encoded in medial prefrontal cortices

We then proceeded to identify the brain regions and timings that encode subjective value during preference-based choice. First, we modelled single trial response-locked neural activity at the sensor level using a GLM (GLM1a, see **Methods**). Given that the subjective values of the chosen ($Chosen_{SV}$) and unchosen ($Unchosen_{SV}$) options (i.e. the likeability ratings provided by participants the day before) predicted preference-based choice (**Fig. 1D**), we used these variables as predictors of the MEG data in preference trials. In order to control for motor response, we added the response button as third control predictor of the neural data. The neural activity over frontal sensors encoded the subjective value of the chosen option in two neighbouring time-windows ($ß_{ChosenSV}$, first cluster: -580 to -370 ms before response, sum(t)=-7613, Monte Carlo p = 0.004. Second cluster: -336 to -197 ms before response, sum(t) = -4405, Monte Carlo p= 0.033; **Fig. 2D** and **Fig. 2E**). No cluster of neural activity significantly encoded the subjective value of the unchosen option. Motor preparation was encoded later in time in two posterior-parietal clusters of opposite polarities ($ß_{Button\ Press}$, negative cluster: -287 to -28 ms before response, sum(t) = -10918, Monte Carlo p = 0.003; positive cluster: -373 to -196 ms before response, sum(t) = 5848, Monte Carlo p = 0.02).

To identify the cortical regions contributing to the encoding of subjective value at sensor-level, we used the same model (GLM1a) to predict source-reconstructed activity averaged in the pre-identified time-window (-580 to -197 ms before response). A network of medial regions comprising right posterior vmPFC (area 32 and 24, cluster peak at MNI coordinates: [7 40 0]), right dorso-medial

prefrontal cortex (dmPFC, area 8m, [5 30 40]), bilateral occipital poles ([6 -77 11], [-1 -85 16]) and mid-posterior insula ([-34 -27 17]) encoded the subjective value of the chosen option (**Fig. 2F**; **Supplementary Table 4**).

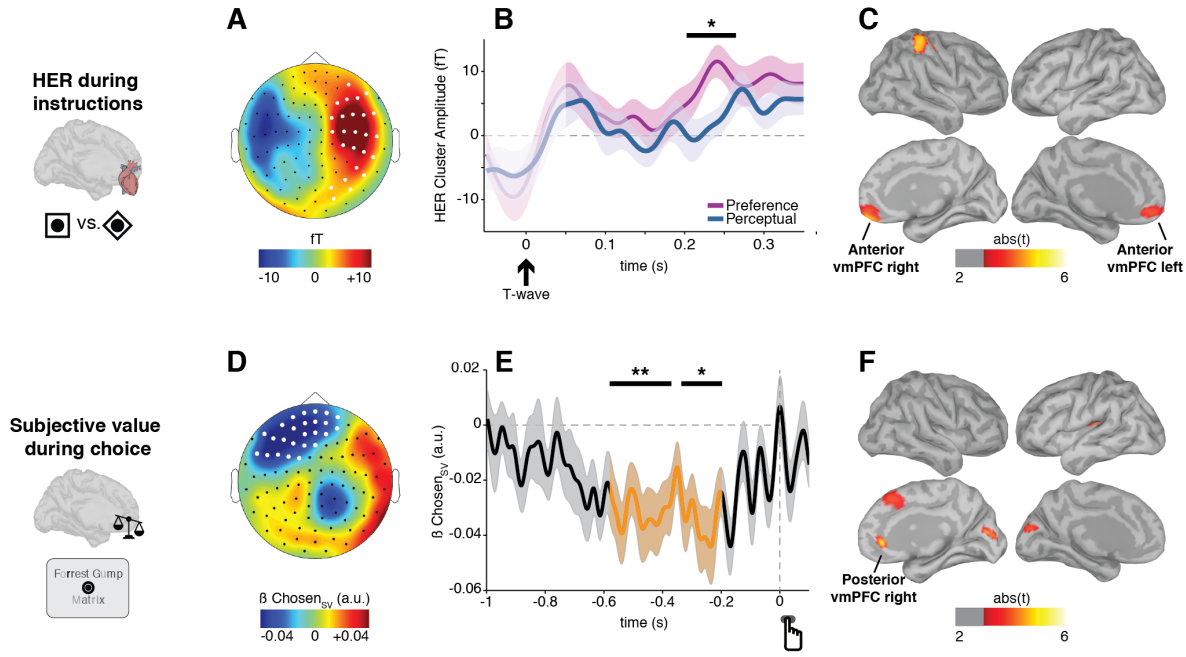

Fig. 2. HERs and subjective value encoding. A, Topography of the significant HER difference between preference-based and perceptual decisions during the instruction period (201-262 ms after T-wave, cluster Monte Carlo p = 0.037). **B**, Time-course of HER (± SEM) for preference-based and perceptual decisions in the cluster highlighted in white in **A**. The portion of the signal (50 ms) still potentially contaminated by the cardiac artifact appears in lighter color. The black bar indicates the significant time-window. **C**, Brain regions mostly contributing to the HER difference between preference-based and perceptual decisions (at least 20 contiguous vertices with uncorrected $p < 0.005$). **D,** Topography of the significant encoding of the subjective value of the chosen option (-580 to -197 ms before response) during choice in preference-based trials. **E**, Time-course (± SEM) of the GLM parameter estimate for the chosen subjective value in the cluster highlighted in white in **D**. Black bars indicate significant time-windows. **F**, Brain regions mostly contributing to the encoding of the subjective value of the chosen option (at least 20 contiguous vertices with uncorrected $p < 0.005$). *p<0.05, **p<0.01.

Table 1. HER difference between preference-based and perceptual decisions. MNI coordinates correspond to the voxel with maximal t-value.

Peak *t* AAL atlas label	Peak *t* MNI coordinates (mm)	*t*-value
R Gyrus Rectus	[1 57 -21]	4.68
L medial orbitofrontal	[-3 47 -6]	3.76
R Post central complex	[32 -22 56]	5.57
R supramarginal gyrus	[41 -33 43]	3.98

HER amplitude modulates trial-by-trial subjective value encoding in right vmPFC

We thus found two effects in two sub-regions of vmPFC. On the one hand, HERs during the instruction period differ when participants prepare for preference-based vs. perceptual decisions in left and right anterior vmPFC. On the other hand, subjective value is encoded during choice in right posterior vmPFC. We then addressed our main question: does the amplitude of neural responses to heartbeats during the instruction period affect the encoding of subjective value during choice in vmPFC (**Fig. 1B**)?

We first focused on right vmPFC, which shows both a differential HER during instructions anteriorly and a parametric encoding of subjective value during choice posteriorly. For each participant, we median-split preference trials into trials with a large HER and small HER based on the activity of anterior r-vmPFC during instruction period. We then determined the strength of subjective value encoding during choice in posterior r-vmPFC by regressing posterior r-vmPFC activity against $\text{Chosen}_{\text{SV}}$, separately for trials with small vs. large HERs. The magnitude of the parameter estimate $ß_{\text{ChosenSV}}$ thus reflects the strength of subjective value encoding.

This analysis revealed (**Fig. 3A**) that the strength of subjective value encoding was significantly modulated by HERs, with greater encoding for large HER trials compared to small HER trials (two-tailed paired t-test on $ß_{ChosenSV}$ in large vs. small HER trials, $t_{(20)}$ = 2.52, p = 0.02). This interaction was confined to the right hemisphere: HER amplitude during instruction presentation in left anterior vmPFC did not influence subjective value encoding in right posterior vmPFC during choice (median split of trials according to HERs amplitude in left anterior vmPFC, comparison of $ß_{ChosenSV}$ in right vmPFC, two-tailed paired t-test, $t_{(20)}$ = 0.83, p = 0.42, BF = 0.40). It is relevant to note that HER amplitude did not vary with pupil diameter or alpha power during choice (**Supplementary Table 5**), indicating that encoding strength is not driven by an overall change in brain state. In addition, the influence of HER amplitude was specific to value encoding since it did not affect the visual responses evoked by option presentation (**Supplementary Table 5**).

The interaction between HER amplitude and subjective value encoding in right vmPFC was also apparent when using a parametric approach. In this GLM (GLM2), we predict the activity of posterior r-vmPFC during choice from the subjective value of the chosen option, the HER amplitude in anterior r-vmPFC during instruction period and the interaction between these two terms (**Fig. 3B**). Since the posterior vmPFC region of interest was defined based on its encoding of the chosen value, the parameter estimate for chosen value was, as expected, large ($ß_{ChosenSV}$ = -0.06 ± 0.02, two-tailed t-test against 0, $t_{(20)}$ = -3.37, p = 0.003). Activity in posterior vmPFC was also influenced by HERs occurring about 1.5 s earlier, during the instruction period, independently from the chosen value ($ß_{HER}$ = 0.04 ± 0.02,

two-tailed t-test against 0, $t_{(20)}$= 2.13, p = 0.046). Importantly, HER and chosen value significantly interacted ($ß_{HER* ChosenSV}$ = -0.05 ± 0.02, two-tailed t-test against 0, $t_{(20)}$= -2.41, p = 0.025). Both the median-split analysis and the parametric model thus reveal a significant interaction between the amplitude of HERs during instruction period and the neural encoding of subjective value during choice.

We then verified that the effect on the neural encoding of subjective value was specific to HER amplitude, and not due to an overall baseline shift in anterior r-vmPFC during the instruction period. We ran an alternative model (GLM3) in which the activity in posterior r-vmPFC was predicted by the subjective value of the chosen option, the activity in anterior r-vmPFC averaged during the whole instruction period, i.e. not time-locked to heartbeats, and the interaction between the two terms. This analysis revealed that while the subjective value of the chosen option significantly predicted the activity of posterior r-vmPFC ($ß_{ChosenSV}$ = -0.05 ± 0.02, two-tailed t-test against 0, $t_{(20)}$ = -3.27, p = 0.004), the other two terms did not (activity in anterior r-vmPFC averaged during instruction period: $ß_{BL\ vmPFC}$ = 0.006 ± 0.03, two-tailed t-test against 0, $t_{(20)}$ = 0.22, p = 0.83, BF = 0.25; interaction: $ß_{BL\ vmPFC* ChosenSV}$ -0.03 ± 0.02, two-tailed t-test against 0, $t_{(20)}$ = -1.55, p = 0.14, BF = 1.14). The encoding of subjective value is thus specifically modulated by HER amplitude in anterior r-vmPFC and not by an overall baseline shift unrelated to heartbeats in the same region.

The functional coupling between HERs and subjective value encoding was also region specific: HER amplitude in anterior r-vmPFC did not modulate the strength of value encoding in any other value-related regions (dmPFC, occipital

poles and posterior insula; all $p \geq 0.13$, all BF ≤ 0.81; **Supplementary Table 6**). In addition, HERs outside anterior r-vmPFC did not interact with value encoding in posterior r-vmPFC. Splitting the trials based on the amplitude in the two other cortical regions showing differential heartbeats-evoked responses (**Fig. 2C**) showed no significant modulation of value encoding (post-central complex: two-tailed paired t-test, $t_{(20)}= -1.41$, $p = 0.17$, BF = 0.90; right supramarginal gyrus: two-tailed paired t-test, $t_{(20)}= -1.96$, $p = 0.06$, BF = 2.41).

The interaction between HER and value encoding affects choice consistency

Is the interaction between HER and value encoding in vmPFC related to behavior? We first tested whether the interaction between HER and value encoding relates to inter-individual differences in choice consistency, i.e. whether participants selected the movie to which they had attributed the greatest likeability rating the day before. Given the overall high performance in preference-based decisions, which may reduce our ability to detect significant relationships, we computed mean choice consistency using the top-50% most difficult trials (i.e. trials above median difficulty in each participant). We regressed the parameter of the interaction between HER and value encoding ($ß_{HER*ChosenSV}$ obtained from GLM2) against mean choice consistency across participants. The larger the interaction between HER and value encoding, the more consistent were participants in their choices ($ß_{robust}$ = 0.41, $R^2 = 0.22$, $t_{(19)} = 2.29$, $p = 0.03$; **Fig. 3C**). In other words, 22% of inter-individual difference in behavioral consistency is explained by the magnitude of the interaction between HER and value encoding. This correlation with behavior was specific to the

interaction parameter: inter-individual differences in choice consistency could not be predicted from the parameter estimate of HER ($ß_{HER}$ from GLM2; $ß_{robust}$ = 0.02, R^2 = $4*10^{-4}$, $t_{(19)}$ = 0.09, p = 0.93, BF = 0.39), nor from the parameter estimate of value ($ß_{ChosenSV}$ from GLM2; $ß_{robust}$ = -0.19, R^2 = 0.04, $t_{(19)}$ = -0.88, p = 0.39, BF = 0.52). None of the personality traits tested nor interoceptive ability, assessed with the heartbeat counting task, significantly co-varied with the interaction between HER and subjective value encoding (**Supplementary Table 7**).

So far, results are based on parameter estimates computed across trials for a given participant. To assess within-participant trial-by-trial influence of the interaction between HERs and subjective value encoding on behavior we computed the z-scored product of the HER in anterior r-vmPFC and the value-related activity in posterior r-vmPFC. We then median-split the trials according to this product and modelled participants' choices separately for trials with a small vs. large interaction (**Fig. 3D**). When the interaction was large psychometric curves featured a steeper slope, corresponding to an increased choice precision (two-tailed paired t-test, $t_{(20)}$= -2.24, p = 0.037; after removal of the unique outlier with a slope estimate exceeding 3 SD from population mean, $t_{(19)}$ = -3.30, p = 0.003; **Fig. 3E**), while decision criterion was not affected (two-tailed paired t-test, $t_{(20)}$= -1.20, p = 0.25, BF = 0.64; after outlier removal $t_{(19)}$ =-0.96, p = 0.35, BF = 0.46; **Fig. 3E**).

To control for the specificity of the interaction, we estimated the psychometric function on trials median-split on HER amplitude alone but found no difference in choice precision (two-tailed paired t-test, $t_{(20)}$= 0.41, p = 0.69, BF = 0.27) nor criterion (two-tailed paired t-test, $t_{(20)}$= 0.52, p = 0.61, BF = 0.29). Similarly,

median-splitting trials on value-related posterior r-vmPFC activity alone revealed no difference in the psychometric curve (two-tailed paired t-test, slope, $t_{(20)}$= 0.21, p = 0.84, BF = 0.25; criterion: $t_{(20)}$= -0.57, p = 0.58, BF = 0.30). Therefore, our results indicate that trial-by-trial choice precision is specifically modulated by the interaction between HERs in anterior r-vmPFC and value-related activity in posterior r-vmPFC.

Altogether, these results indicate that the interaction between HER amplitude and subjective value encoding accounts both for within-subject inter-trial variability, and for inter-individual differences in preference-based choice consistency.

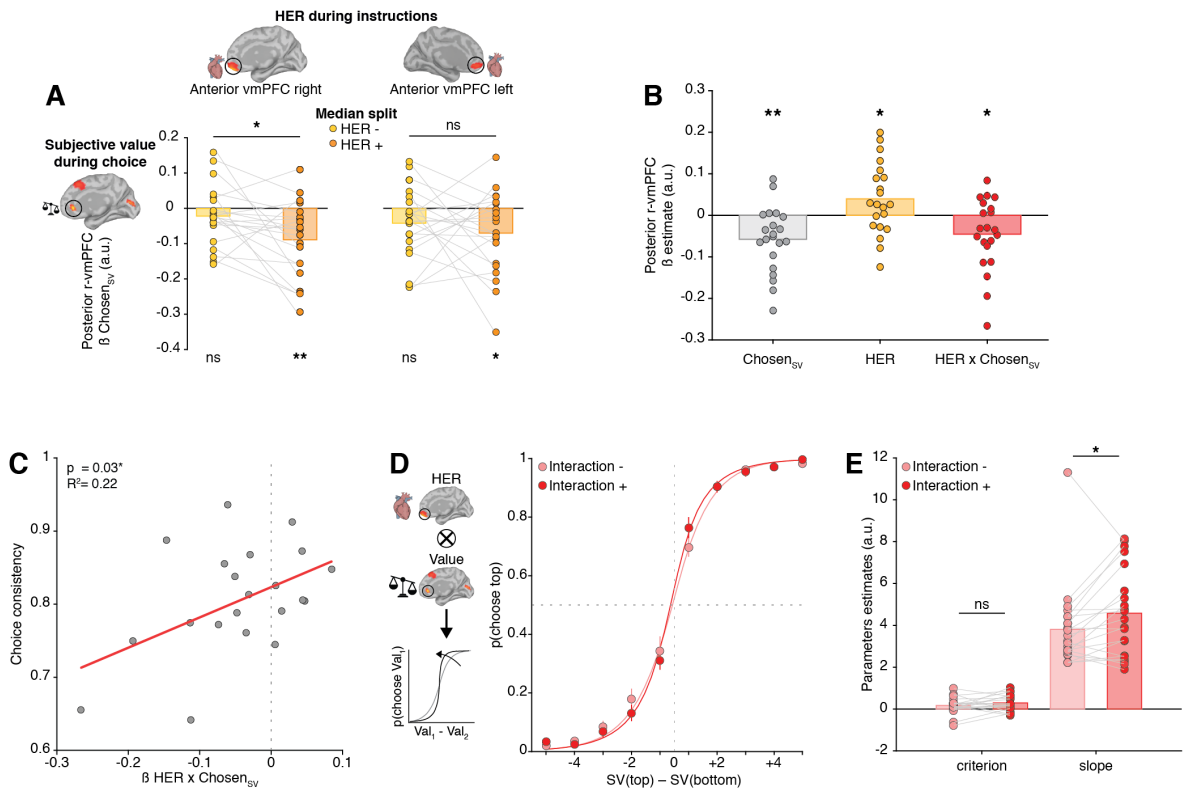

Fig. 3. The interaction between HER and value encoding accounts for inter-individual choice consistency and trial-by-trial intra-individual choice precision. A, Parameter estimates for subjective value of the chosen option in posterior r-vmPFC during choice significantly differ in trials with large vs. small HERs in anterior r-vmPFC during instructions (p = 0.02). **B**, Activity in posterior r-vmPFC depends not only on the subjective value of the chosen option, but also on the HER during instructions and on the interaction between HER and value. **C**, The magnitude of the interaction between HER and value encoding predicts inter-individual variability in choice consistency, with a stronger interaction predicting more consistent choices. **D**, Participants' choices were separately modeled according to the trial-by-trial neural interaction between HER (in anterior r-vmPFC) and subjective value encoding (in posterior r-vmPFC). Lines represent model fit, dots participants' behavior. Error bars represent SEM. **E**, Parameters estimates for the psychometric functions in **D** show a steeper slope for trials with large interaction between HER and value-related vmPFC activity (p = 0.037). Decision criterion is unaffected. *p<0.05, **p<0.01.

HER influence is specific to preference-based choices

Finally, we tested whether the influence of HER was specific to subjective value or whether it is a more general mechanism modulating all types of decision-relevant evidence. To this aim, we analyzed perceptual discrimination trials using the same approach as for preference-based trials. First, we modeled the single trial response-locked MEG sensor-level data using a GLM (GLM1b) with the parameters accounting for choice in the perceptual task (i.e. contrast of the chosen option – $Chosen_{Ctrs}$ – and the contrast of the unchosen option – $Unchosen_{Ctrs}$). Similarly to GLM1a, we included the button used to respond as third predictor to account for motor response. We then identified the time windows where the contrast of the chosen option, unchosen option and response button were encoded (**Supplementary Table 8**) and determined the cortical regions contributing to the encoding of the contrast of the chosen option (**Supplementary Fig. 2, Supplementary Table 9**). Finally, we median-split perceptual trials according to the amplitude of HERs in anterior r-vmPFC. The encoding strength of the contrast of the chosen option did not depend on heart-evoked responses amplitude in any of the contrast-encoding regions (all $p \geq 0.26$, $BF \leq 0.62$; **Supplementary Table 10**). The results thus suggest that HER amplitude in r-vmPFC specifically influences the cortical representation of subjective value.

Discussion

We show that preference-based choice consistency depend on the influence that neural responses to heartbeats exert on value representation in vmPFC. A larger interaction between HER and value encoding benefitted behavior, leading to improved choice precision at the single trial level, and positively correlated with inter-individual choice consistency. Within the valuation network, the interaction between HER and value encoding was specific to vmPFC, a region known to play an integrative role in valuation (Delgado et al., 2016; Fellows, 2006; Vaidya et al., 2017). The effect of HER was absent in the control condition, an objective visual discrimination task.

We successfully retrieved from MEG data the cortical valuation network described in the fMRI literature (Bartra et al., 2013; Clithero and Rangel, 2014; Levy and Glimcher, 2012), including dmPFC and vmPFC, during the choice period. Data on the temporal course of value-based choices in prefrontal cortex remain scarce (Hunt et al., 2012, 2015; Polanía et al., 2014; Rich and Wallis, 2016). Here, we find that the chosen value is robustly encoded in the valuation network from 600 ms to 200 ms before motor response, with a temporal overlap between value encoding and motor preparation. Note that in the preference-based task, we did not find a robust encoding of the unchosen value, in line with electrophysiological recordings in the monkey orbitofrontal cortex where the encoding of the chosen value dominates (Hunt et al., 2015; Padoa-Schioppa and Assad, 2006; Rich and Wallis, 2016; Strait et al., 2014).

HERs were larger when participants prepared to perform subjective, preference-based choices than when participants prepared to perform an objective visual discrimination, in anterior vmPFC and post-central gyrus, two regions known to respond to heartbeats (Babo-Rebelo et al., 2016b, 2016a; Kern et al., 2013; Park et al., 2014). The increase in HERs in the preference task thus appears related to the subjective, self-reflecting component inherent to preference-based choices, in line with theoretical proposals implicating the neural monitoring of bodily states in self-related cognition (Azzalini et al., 2019; Blanke and Metzinger, 2009; Damasio, 2010; Park and Tallon-baudry, 2014). In addition, neither differences in HERs between the objective and subjective tasks, nor the interaction between HERs and subjective value encoding were related to differences in the cardiac parameters measured (heart rate, heart rate variability, ECG, stroke volume). This suggests that in this experiment, fluctuations in HERs and in the interaction between HER and value encoding correspond to changes in the quality of the neural monitoring of cardiac inputs, rather than to actual changes in cardiac inputs.

What is the nature of the interaction between HERs and value encoding in vmPFC? Because fluctuations in HERs occur before option presentation, their influence on value encoding might generally pertain to the interaction between ongoing and stimulus-evoked activity. Still, value encoding specifically interacted with the transient neural activity evoked by heartbeats; no interaction between overall ongoing activity in vmPFC and value encoding could be found. In addition, HERs modulated value encoding in a multiplicative manner. Our results thus differ from a previously reported vmPFC additive baseline-shift affecting pleasantness

ratings (Abitbol et al., 2015). Neither HERs nor the interaction between HERs and value encoding covaried with neural and peripheral markers of arousal. Altogether, these results indicate that fluctuations in HERs and in the interaction between HERs and value encoding do not reflect changes in a global state, but rather are specific to neural responses to heartbeats in vmPFC.

What is the role of HERs in the subjective decision process? Two opposite predictions were initially made. In the first one, HERs would correspond to the mandatory neural monitoring of a physiological variable embedded in the decision process, even when physiology is irrelevant. Under this hypothesis HERs would add noise to the decision and therefore decrease choice precision. Since we found that HERs improved choice precision, our results rather favor the alternative hypothesis that HERs convey a beneficial component, specifically related to subjective decisions. HERs, through their interaction with value encoding, led to choices that were more consistent with the likability ratings that participants provided the day before the experiment. HERs in vmPFC thus support the subjective valuation process, potentially by stabilizing the self-representation of the decision-maker (Azzalini et al., 2019; Park and Tallon-baudry, 2014) necessary for subjective valuation, in line with the role of vmPFC in integrating physiological signals in rational decision-making (Bechara et al., 1997; De Martino et al., 2006).

The integration of physiological variables in the valuation of primary goods such as food items has obvious ecological relevance. Our results reveal that the valuation of cultural goods, devoid of any immediate physiological consequence, has inherited this tight link with the homeostatic neural circuitry. This inheritance

benefits behavior, as a larger influence of HERs on value encoding led to more consistent choices. Noise in neural activity has long been considered as a likely candidate accounting for fluctuations in choice consistency (Abitbol et al., 2015; Fehr and Rangel, 2011; Findling et al.; Kurtz-David et al., 2019; Padoa-Schioppa, 2013; Polanía et al., 2014). We specify here the nature of (a portion of) this underspecified noise in preference-based choices: it stems from the homeostatic monitoring of physiological variables, that when reduced, leads to inconsistent, or irrational, choices.

Acknowledgements

The authors thank Clémence Alméras, Maximilien Chaumon and Christophe Gitton for assistance in data acquisition.

This work was supported by funding from the European Research Council (ERC) under the European Union's Horizon 2020 research and innovation program (grant agreement No 670325, Advanced grant BRAVIUS) and a senior fellowship of the Canadian Institute For Advance Research (CIFAR) program in Brain, Mind and Consciousness to CTB; by a grant from the Ecole des Neurosciences de Paris Ile de France to DA; and by ANR-17-EURE-0017.

Author contributions

DA, SP and CTB designed the study. DA collected the data. DA, CTB and AB analyzed the data. DA and CTB interpreted the results and wrote the first draft of the paper. All authors contributed to the final version of the paper.

Declaration of interests

The authors declare no competing interests.

Code and data availability

The custom code used for the main analyses of this paper can be accessed online at https://github.com/DamianoAzzalini/HER-preferences.

The data that support the findings of this study will be available from the corresponding authors upon reasonable request, once the paper is published in a peer-reviewed journal.

Methods

Participants

24 right-handed volunteers with normal or corrected-to-normal vision took part in the study after having given written informed consent. They received monetary compensation for their participation. The ethics committee CPP Ile de France III approved all experimental procedures. Three subjects were excluded from analysis: one subject for too low overall performance (74%, 2 standard deviations below the mean = 87.6%), one subject was excluded for excessive number of artifacts (29.7% of trials, above 2 standard deviations, mean = 7%), one subject was excluded because the ICA correction of the cardiac artifact was not successful.

21 subjects were thus retained for all subsequent analyses (9 male; mean age: 23.57 ± 2.4 years; mean ± SD).

Tasks and procedure

Participants came on two consecutive days to the lab (mean elapsed time between the two sessions 22.28 ± 3.55 hours) to complete two experimental sessions. The first session was a likability rating behavioral session on movies, from which we drew the stimuli used in the second experimental session, during which brain activity was recorded with magnetoencephalography (MEG).

Rating session. We selected 540 popular movies form the Web (allocine.fr) whose title maximal length was 16 characters (spaces included). DVD covers and titles of the pre-selected movies were displayed one by one on a computer screen

and subjects had to indicate whether they had previously watched the currently displayed movie by pressing a 'yes' or 'no' key on a computer keyboard, without any time constrain (**Supplementary Fig. 1A**). Participants were then presented with the list of movie titles they had previously watched and asked to name the 2 movies they liked the most and the two they liked the least. Participants were explicitly instructed to use these 4 movies as reference points (the extremes of the rating scale) to rate all other movies. Last, the titles and the covers of the movies belonging to the list were displayed one by one at the center of the computer screen in random order. Participants assigned to each movie a likability rating by displacing (with arrow keys) a cursor on a 21-points Likert scale and validated their choice with an additional button press (**Supplementary Fig. 1B**). Likability ratings were self-paced and the starting position of the cursor was randomized at every trial.

Stimuli. Experimental stimuli consisted of 256 pairs of written movie titles drawn from the list of movies that each participant had rated on the first day. Each movie title was characterized along two experimental dimensions: its likability rating (as provided by the participant) and its contrast. The mean contrast was obtained by averaging the luminance value (between 40 and 100; grey background at 190) randomly assigned to each character of the title. We manipulated trials difficulty by pairing movie titles so that the differences between the two items along the two dimensions (i.e., likability and contrast) were parametric and orthogonal. Additionally, we controlled that the sum of ratings and the sum of contrast within each difficulty level was independent of their difference and evenly distributed. Each pair of stimuli was presented twice in the experiment: one per decision type. A

given movie title could appear in up to 10 different pairs. The position of the movie titles on the screen was pseudo-randomly assigned so that the position of the correct option (higher likeability rating or higher contrast) was fully counter-balanced.

Experimental task. On the second day, subjects performed a two-alternative forced-choice (2AFC) task while brain activity was recorded with MEG. At each trial, participants were instructed to perform one of the two decisions types on the pair of movie titles (**Fig. 1A**): either a preference decision, in which they had to indicate the item they liked the most, or a perceptual discrimination, in which they had to indicate the title written with the higher contrast. Each trial began with a fixation period of variable duration (uniformly distributed between 0.8 and 1.2 seconds in step of 0.05 s) indicated by a black fixation dot surrounded by a black ring (internal dot, 0.20° of visual angle; external black ring, 0.40° of visual angle), starting from which participants were required not to blink anymore. Next, the outer ring of the fixation turned either into a square or a diamond (0.40° and 0.56° visual angle, respectively) indicating which type of decision participants were to perform (preference-based or perceptual, counter-balanced across participants), for 1.5 seconds. Then, the outer shape turned again into a ring and two movie titles appeared above and below it (visual angle 1.09°). Options remained on screen until response was provided (via button press with the right hand) or until 3 seconds had elapsed. After response delivery, movie titles disappeared and the black fixation dot surrounded by the black circle remained on screen for 1 more second. The central dot turned green and stayed on screen for variable time (uniformly distributed between 2.5 and 3 seconds in step of 0.05 s), indicating participants that they were

allowed to blink before the beginning of next trial. Each recording session consisted of 8 blocks of 64 trials each.

Prior to the recording session, participants familiarized themselves with the experimental task by carrying out 3 training blocks. The first 2 blocks (10 trials each) comprised trials of one type only, hence preceded by the same cue symbol. The last block contained interleaved trials (n=20), as in the actual recording. The movie pairs used during training were not presented again during the recording session.

Heartbeat counting task. After performing the 8 experimental blocks, we assessed participants' interoceptive abilities by asking them to count their heartbeats by focusing on their bodily sensations, while fixating the screen (Schandry, 1981). Subjects performed six blocks of different durations (30, 45, 60, 80, 100, 120 seconds) in randomized order. No feedback on performance was provided. Since the acquisition of our dataset, this widely used paradigm has been criticized in several respects (Desmedt et al., 2018; Ring et al., 2015; Zamariola et al., 2018).

Questionnaires. Once subjects left the MEG room, they filled 4 questionnaires in French: Beck's Depression Inventory (BDI) (Beck et al., 1961), Peter's et al. Delusions Inventory (PDI) (Peters et al., 2004), the Trait Anxiety Inventory (STAI) (Spielberger et al., 1983) and the Obsessive-Compulsive Inventory (OCI) (Foa et al., 2002).

Recordings

Neural activity was continuously recorded using a MEG system with 102 magnetometers and 204 planar gradiometers (Elekta Neuromag TRIUX, sampling rate 1000 Hz, online low-pass filter at 330 Hz). Cardiac activity was simultaneously

recorded (BIOPAC Systems, Inc.; sampling frequency 1000 Hz; online filter 0.05-35 Hz). The electrocardiogram was obtained from 4 electrodes (2 placed in over the left and right clavicles, 2 over left and right supraspinatus muscles (Gray et al., 2007)) and referenced to another electrode on the left iliac region of the abdomen, corresponding to four vertical derivations. The four horizontal derivations were computed offline by subtracting the activity of two adjacent electrodes. Additionally, we measured beat-to-beat changes in cardiac impedance, to compute the beat-by-beat stroke volume (i.e. the volume of blood ejected by the heart at each heartbeat (Kubicek et al., 1970)). Impedance cardiography is a non-invasive technique based on the impedance changes in the thorax due to the changes in fluid volume (blood). A very low-intensity (400 μA rms) high frequency (12.5 kHz) electric current was injected via two source electrodes: the first one was placed on the left side of the neck and the second 30 cm below it (roughly on the sixth rib). Two other monitoring electrodes (placed 4 cm apart from the source ones: below the source electrode on the neck and above the source electrode on the rib cage) measured the voltage across the tissue. To determine left ventricular ejection time, aortic valve activity was recorded by placing an a-magnetic homemade microphone (online band-pass filter 0.05-300 Hz) on the chest of the subject.

Pupil diameter and eye movements were tracked using an eye-tracker device (EyeLink 1000, SR Research) and 4 electrodes (2 electrodes placed on the left and right temples and 2 electrodes placed above and below participant's dominant eye).

Cardiac events and parameters

Cardiac events were detected on the right clavicle-left abdomen ECG derivation in all participants. We computed a template of the cardiac cycle, by averaging a subset of cardiac cycles, which was then convolved with the ECG time series. R-peaks were identified as peaks of the result of the convolution, normalized between 0 and 1, exceeding 0.6. All other cardiac waves were defined with respect R-peak. In particular, T-waves were identified as the maximum amplitude occurring within 420 milliseconds after the Q-wave. R-peak and T-wave automatic detection was visually verified for each participant.

Inter-beat intervals (IBIs) were defined for each phase of the trial as the intervals between two consecutive R-peaks. More specifically, we considered for 'fixation', 'instruction period' and 'response' phases the two R-peaks around their occurrence. IBIs during 'choice' were based on the two R-peaks preceding response delivery. Inter-beat variability was defined as the standard deviation across trials of IBIs in a given trial phase.

Stroke volume was computed according to the formula (Kubicek et al., 1970; Sherwood et al., 1990):

$$SV = \rho \times \left(\frac{L^2}{Zo^2}\right) \times LVET \times \frac{dZ}{dT_{(max)}}$$

where ρ is the resistivity of the blood (135 Ohms*cm) (Berntson et al., 2007), L^2 is the distance between the two source electrodes, Zo^2 is the base impedance, $LVET$ is the systolic left ventricular ejection time (in seconds), $dZ/dT_{(max)}$ is the largest impedance change during systole (Ohms/sec). Note that because we obtained stroke volume by injecting a current at 12.5 kHz, rather than the more typical frequency of 100 kHz, absolute stroke volumes are systematically underestimated, but relative values are preserved.

MEG data preprocessing

External noise was removed from the continuous data using MaxFilter algorithm. Continuous data were then high-pass filtered at 0.5 Hz (4th order Butterworth filter). Trials (defined as epochs ranging from fixation period to 1 second after response) contaminated by muscle and movement artifacts were manually identified and discarded from further analyses (6% of trials on average, ranging from 0% to 15%).

Independent component analysis (ICA) (Delorme and Makeig, 2004), as implemented in FieldTrip Toolbox (Oostenveld et al., 2011) was used to attenuate the cardiac artifact on MEG data. ICA was computed on MEG data epoched ±200 ms around the R-peak of the ECG, in data segments that were free of artifacts, blinks and saccades above 3 degrees. The number of independent components to compute was set to be equal to the rank of the MEG data. Mean pairwise phase consistency (PPC) was estimated for each independent component(Vinck et al., 2010) with the right clavicle-left abdomen ECG derivation signal in the frequency band 0-25 Hz. Components (up to 3) that exceeded 3 standard deviations from mean PPC were then removed from the continuous data.

To correct for blinks, 2-seconds segments of data were used to estimate blink and eye-movement components. Mean PCC was then computed with respect to vertical EOG signal, and components exceeding mean PCC + 3 standard deviations were removed from continuous data. The procedure was iterated until no component was beyond 3 standard deviations or until 3 components in total were

removed. Stereotypical blink components were manually selected in two participants as the automated procedure failed to identified them.

ICA-corrected data were then low-pass filtered at 25 Hz (6th order Butterworth filter)

Trials selection

Trials had to meet the following criteria to be included in all subsequent analysis: no movement artifacts, sum of blinking periods less than 20% of total trial time, at least one T-peak during instruction period (cf. HERs section), and reaction time neither too short (at least 250 ms) nor too long. To identify exceedingly long RTs, we binned the trials of each task in 4 difficulty levels based on the difference of the two options (i.e., difference in ratings in preference-based choice and difference in contrast for the perceptual ones). Within each difficulty level, for correct and error trials separately, we excluded the trials with reaction times exceeding the participant's mean RT + 2 standard deviations.

The average number of trials retained per participant was 421.67 ± 43.36 (mean ± SD).

Heartbeat evoked responses

Heart-evoked responses were computed on MEG data time-locked to T-wave occurring during the instruction period. T-waves had to be at minimum 400 ms distance from the subsequent R-peak. In order to avoid contamination by transient visual responses or by preparation to the subsequent visual presentation, we only retained T-waves that occurred at least 300 milliseconds after the onset of

the instruction cue and 350 milliseconds before the onset of options presentation. If more than one T-wave occurred in this period, HERs for that trial were averaged. HERs were analyzed from T-wave + 50 ms to minimize contamination by the residual cardiac artifact (Dirlich et al., 1997) after ICA correction.

We verify that differences in HERs between the two types of decision were truly locked to heartbeats, and that a difference of similar magnitude could not arise by locking the data to any time point of the instruction period. To this end, we created surrogate timings for heartbeats (within the instruction period), to break the temporal relationship between neural data and heartbeats, and computed surrogate HERs. We created 500 surrogate heartbeat data set, by permuting the timings of the real T-wave between trials belonging to the same decision type (i.e., the timing of the T-wave at trial *i* was randomly assigned to trial *j*). We then searched for surrogate HER differences between trial types using a cluster-based permutation test (Maris and Oostenveld, 2007) (see below). For each of the 500 iterations, we retained the value of the largest cluster statistics (sum(t)) to estimate the distribution of the largest difference that could be obtained randomly sampling ongoing neural activity during the same instruction period. To assess statistical significance, we compared the cluster statistics from the original data against the distribution of surrogate statistics.

Nonparametric statistical testing of MEG data

HERs difference between preference-based and perceptual trials during instruction presentation was tested for statistical significance using cluster-based permutation two-tailed t-test (Maris and Oostenveld, 2007) as implemented in

FieldTrip toolbox (Oostenveld et al., 2011), on magnetometer activity in the time-window 50-300 ms after T-wave. This method defines candidate clusters of neural activity based on spatio-temporal adjacency exceeding a statistical threshold ($p < 0.05$) for a given number of neighboring sensors (n=3). Each candidate cluster is assigned a cluster-level test statistics corresponding to the sum of *t* values of all samples belonging to the given cluster. The null distribution is obtained non-parametrically by randomly shuffling conditions labels 10,000 times, computing at each iteration the cluster statistics and saving the largest positive and negative *t* sum. Monte Carlo p value corresponds to the proportion of cluster statistics under the null distribution that exceed the original cluster-level test statistics. Because the largest chance values are retained to construct the null distribution, this method intrinsically corrects for multiple comparisons across time and space. Controls analyses involving the clustering procedure were performed with the same parameters.

The significance of beta time-series obtained from GLM analyses at the sensor level was obtained using cluster-based permutation two-tailed t-test against zero.

Bayes factor

We used Bayes factors (BF) to quantify the evidence in support of the null hypothesis (H_0 = no difference between 2 measures). To this aim, we computed the maximum log-likelihood of a gaussian model in favor of the alternative hypothesis and for the model favoring the null adjusting the effect size to correspond to a $p = 0.05$ for our sample size (n = 21 for all analyses except for pupil for which n = 16

and for 3 ECG derivations for which n=20). Finally, we computed Bayesian information criterion and the corresponding Bayes factor. As a summary indication, BF < 0.33 provides substantial evidence in favor of the null hypothesis, BF between 0.33 and 3 does not provide enough evidence for or against the null (Kass and Raftery, 1995).

For regression analyses, Bayes Factor was computed using the online calculator tool (http://pcl.missouri.edu/bf-reg) based on Liang and colleagues (Liang et al., 2008).

Generalized linear model on response-locked single trials

To analyze how task-related variables are encoded in neural activity during decision, we ran a generalized linear model (GLM) on baseline-corrected (-500 to -200 ms before instruction presentation) single trial MEG data time-locked to button press. We predicted z-scored MEG activity at each time-point and channel using task-relevant experimental variables. For preference-based decisions we modeled MEG activity as:

$$MEG_{t,c} = \beta_0 + \beta_{ChosenSV} + \beta_{UnchosenSV} + \beta_{Button\ press}\ (GLM1a)$$

where t and c represent MEG activity at time-point t at channel c, β_0 is the intercept, $\beta_{ChosenSV}$ are the z-scored ratings of the chosen option, $\beta_{UnchosenSV}$ is the z-scored rating of the alternative unchosen option and $\beta_{Button\ press}$ is a categorical variable representing motor response (i.e. top or bottom). Similarly, for perceptual decisions we used:

$$MEG_{t,c} = \beta_0 + \beta_{ChosenCtrs} + \beta_{UnchosenCtrs} + \beta_{Button\ press}\ (GLM1b)$$

where $\beta_{ChosenCtrs}$ and $\beta_{UnchosenCtrs}$ are the z-scored contrast of the chosen and unchosen option, respectively.

This procedure provided us with time series of beta values at each channel that could be tested against zero for significance using spatio-temporal clustering (Maris and Oostenveld, 2007). Once significant clusters encoding task-related variables were identified at the sensor level, we reconstructed the cortical sources corresponding to the sensor-level activity averaged within the significant time-window. We modeled source-reconstructed neural activity with the same GLMs to identify the cortical areas mostly contributing to the significant sensor-level effect.

Generalized linear model on posterior right vmPFC

To quantify the influence of HER in anterior r-vmPFC during instructions on subjective value encoding during choice, we modeled the activity of posterior r-vmPFC, encoding subjective value with the following GLM:

$$Posterior\ r\text{-}vmPFC = \beta_0 + \beta_{Chosen\mathrm{SV}} + \beta_{HER} + \beta_{\mathrm{HER*ChosenSV}}\ (GLM2)$$

where, β_0 is the intercept, $\beta_{Chosen\mathrm{SV}}$ are the z-scored ratings of the chosen option, β_{HER} is the z-scored activity in the anterior right vmPFC cluster defined by comparing HERs in preference-based vs. perceptual choices and $\beta_{Chosen\mathrm{SV*HER}}$ is the interaction term obtained by multiplying the z-scored previous predictors.

To verify that the interaction between subjective value encoding and HER amplitude was specifically time-locked to heartbeats and not a general influence of

baseline activity in anterior r-vmPFC, we ran an alternative model to explain posterior r-vmPFC activity:

$$Posterior\ r\text{–}\ vmPFC = \beta_0 + \beta_{Chosen\mathrm{SV}} + \beta_{BL\ vmPFC} + \beta_{BL\ vmPFC*ChosenSV}\ (GLM3)$$

where, β_0 is the intercept, $\beta_{Chosen\mathrm{SV}}$ are the z-scored ratings of the chosen option, $\beta_{BL\ vmPFC}$ is the z-scored activity in anterior r-vmPFC during instructions averaged across the whole instruction period, not time-locked to heartbeats and $\beta_{BL\ vmPFC*ChosenSV}$ is the interaction between the two preceding predictors.

Note that regressors are not orthogonalized in any of the GLMs.

Anatomical MR acquisition and preprocessing

An anatomical T1 scan was acquired for each participant on a 3 Tesla Siemens TRIO (n = 2) or Siemens PRISMA (n = 20) or Siemens VERIO (n = 2). Cortical segmentation was obtained by using automated procedure as implemented in the FreeSurfer software package (Fischl et al., 2004). The results were visually inspected and used for minimum-norm estimation.

Source reconstruction

Cortical localization of neural activity was performed with BrainStorm toolbox (Tadel et al., 2011). After co-registration of individual anatomy and MEG sensors, 15,003 current dipoles were estimated using a linear inverse solution from time-series of magnetometers and planar gradiometers (weighted minimum-norm, SNR of 3, whitening PCA, depth weighting of 0.5) using overlapping-spheres head

model. Current dipoles were constrained to be normally oriented to cortical surface, based on individual anatomy. Source activity was obtained by averaging sensor-level time-series in the time-windows showing significant effects (difference between HERs and beta values different from zero), spatially smoothed (FWHM 6 mm) and projected onto standard brain model (ICBM152_T1, 15,003 vertices). Note that sources in subcortical regions cannot be retrieved with the reconstruction method used here.

To assess which cortical areas contributed the most to the effects observed at the sensor-level, we ran parametric two-tailed t-test and reported all clusters of activity spatially extending more than 20 vertices with individual t-values corresponding to $p < 0.005$ (uncorrected for multiple comparisons). We reported the coordinates of vertices with the maximal t value and their anatomical labels according to AAL atlas (Tzourio-Mazoyer et al., 2002). For clusters falling into prefrontal cortices, we reported the corresponding areas according to the connectivity-based parcellation developed by Neubert and colleagues (Neubert et al., 2015).

Pupil data analysis

Pupil data that contained blinks (automatically detected with EyeLink software and extended before and after by 150 ms), saccades beyond 2 degrees and segments in which pupil size changed abruptly (signal temporal derivative exceeding 0.3, arbitrary unit) were linearly interpolated. All interpolated portions of the data that exceeded 1 second were removed from further analyses. Continuous pupil data from each experimental block were then band-pass filtered between 0.01

and 10 Hz (second order Butterworth) and z-scored. 16 subjects were retained for pupil analysis; 5 subjects were excluded due to too low quality of data. Pupil analysis was performed in two ways: 1) averaged pupil diameter in the same time period used for HER computation (i.e., 300 ms after instruction presentation until 350 ms before options display) and 2) averaged pupil diameter in the time-window spanning 1 second before button press until its execution.

References:

Abitbol, R., Lebreton, M., Hollard, G., Richmond, B.J., Bouret, S., and Pessiglione, M. (2015). Neural Mechanisms Underlying Contextual Dependency of Subjective Values: Converging Evidence from Monkeys and Humans. J. Neurosci. *35*, 2308–2320.

Azzalini, D., Rebollo, I., and Tallon-Baudry, C. (2019). Visceral Signals Shape Brain Dynamics and Cognition. Trends Cogn. Sci. *23*, 488–509.

Babo-Rebelo, M., Richter, C.G., and Tallon-Baudry, C. (2016a). Neural Responses to Heartbeats in the Default Network Encode the Self in Spontaneous Thoughts. J. Neurosci. *36*, 7829–7840.

Babo-Rebelo, M., Wolpert, N., Adam, C., Hasboun, D., and Tallon-Baudry, C. (2016b). Is the cardiac monitoring function related to the self in both the default network and right anterior insula? Philos. Trans. R. Soc. B Biol. Sci. *371*, 20160004.

Bartra, O., McGuire, J.T., and Kable, J.W. (2013). The valuation system: A coordinate-based meta-analysis of BOLD fMRI experiments examining neural correlates of subjective value. Neuroimage *76*, 412–427.

Bechara, A., Damasio, H., Tranel, D., and Damasio, A.R. (1997). Deciding Advantageously Before Knowing the Advantageous Strategy. Science (80-.). *275*, 1293–1295.

Beck, A., Ward, C.H., Mendelson, M., Mock, J., and Erbaught, J. (1961). An Inventory for Measuring Depression. Arch. Gen. Psychiatry *4*, 561–571.

Berntson, G.G., Quigley, K.S., and Lozano, D. (2007). Cardiovascular Psychophysiology. In Handbook of Psychophysiology, J.T. Cacioppo, L.G. Tassinary, and G. Berntson, eds. (Cambridge University Press), pp. 182–210.

Berthoud, H.R. (2011). Metabolic and hedonic drives in the neural control of appetite: Who is the boss? Curr. Opin. Neurobiol. *21*, 888–896.

Blanke, O., and Metzinger, T. (2009). Full-body illusions and minimal phenomenal selfhood. Trends Cogn. Sci. *13*, 7–13.

Blanke, O., Slater, M., and Serino, A. (2015). Behavioral, Neural, and Computational Principles of Bodily Self-Consciousness. Neuron *88*, 145–166.

Chib, V.S., Rangel, A., Shimojo, S., and O'Doherty, J.P. (2009). Evidence for a Common Representation of Decision Values for Dissimilar Goods in Human Ventromedial Prefrontal Cortex. J. Neurosci. *29*, 12315–12320.

Clithero, J.A., and Rangel, A. (2014). Informatic parcellation of the network involved in the computation of subjective value. Soc. Cogn. Affect. Neurosci. *9*, 1289–1302.

Damasio, A.R. (2010). Self Comes to Mind: Constructing the Conscious Brain (Pantheon Books).

Delgado, M.R., Beer, J.S., Fellows, L.K., Huettel, S.A., Platt, M.L., Quirk, G.J., and Schiller, D. (2016). Viewpoints: Dialogues on the functional role of the ventromedial prefrontal cortex. Nat. Neurosci. *19*, 1545–1552.

Delorme, A., and Makeig, S. (2004). EEGLAB: an open source toolbox for analysis of single-trial EEG dynamics including independent component analysis. J. Neurosci. Methods *134*, 9–21.

Desmedt, O., Luminet, O., and Corneille, O. (2018). The heartbeat counting task largely involves non-interoceptive processes: Evidence from both the original and an adapted counting task. Biol. Psychol. *138*, 185–188.

Dirlich, G., Vogl, L., Plaschke, M., and Strian, F. (1997). Cardiac field effects on the EEG. Electroencephalogr. Clin. Neurophysiol. *102*, 307–315.

Fehr, E., and Rangel, A. (2011). Neuroeconomic Foundations of Economic Choice—Recent Advances. J. Econ. Perspect. *25*, 3–30.

Fellows, L.K. (2006). Deciding how to decide: Ventromedial frontal lobe damage affects information acquisition in multi-attribute decision making. Brain *129*, 944–952.

Findling, C., Skvortsova, V., Dromnelle, R., Palminteri, S., and Wyart, V. Computational noise in reward-guided learning drives behavioral variability in volatile environments. Nat. Neurosci. *in press*.

Fischl, B., Van Der Kouwe, A., Destrieux, C., Halgren, E., Ségonne, F., Salat, D.H., Busa, E., Seidman, L.J., Goldstein, J., Kennedy, D., et al. (2004). Automatically Parcellating the Human Cerebral Cortex. Cereb. Cortex *14*, 11–22.

Foa, E.B., Huppert, J.D., Leiberg, S., Langner, R., Kichic, R., Hajcak, G., and Salkovskis, P.M. (2002). The Obsessive-Compulsive Inventory: Development and validation of a short version. Psychol. Assess. *14*, 485–496.

Gray, M.A., Taggart, P., Sutton, P.M., Groves, D., Holdright, D.R., Bradbury, D., Brull, D., and Critchley, H.D. (2007). A cortical potential reflecting cardiac function. PNAS *104*, 6818–6823.

Hunt, L.T., Kolling, N., Soltani, A., Woolrich, M.W., Rushworth, M.F.S., and Behrens, T.E.J. (2012). Mechanisms underlying cortical activity during value-guided choice. Nat. Neurosci. *15*, 470–476.

Hunt, L.T., Behrens, T.E.J., Hosokawa, T., Wallis, J.D., and Kennerley, S.W. (2015). Capturing the temporal evolution of choice across prefrontal cortex. Elife *4*, 1–25.

Juechems, K., and Summerfield, C. (2019). Where does value come from? Trends Cogn. Sci. 836–850.

Kass, R.E., and Raftery, A.E. (1995). Bayes factors. J. Am. Stat. Assoc. *90*, 773–795.

Keramati, M., and Gutkin, B. (2014). Homeostatic reinforcement learning for integrating reward collection and physiological stability. Elife *3*, 1–26.

Kern, M., Aertsen, A., Schulze-Bonhage, A., and Ball, T. (2013). Heart cycle-related effects on event-related potentials, spectral power changes, and connectivity patterns in the human ECoG. Neuroimage *81*, 178–190.

Kubicek, W.G., Patterson, R.P., and Witsoe, D.A. (1970). Impedance Cardiography As a Noninvasive Method of Monitoring Cardiac Function and Other Parameters of the Cardiovascular System. Ann. N. Y. Acad. Sci. *170*, 724–732.

Kurtz-David, V., Persitz, D., Webb, R., and Levy, D.J. (2019). The neural computation of inconsistent choice behavior. Nat. Commun. *10*, 1583.

Lebreton, M., Jorge, S., Michel, V., Thirion, B., and Pessiglione, M. (2009). An Automatic Valuation System in the Human Brain: Evidence from Functional Neuroimaging. Neuron *64*, 431–439.

Levy, D.J., and Glimcher, P.W. (2011). Comparing Apples and Oranges: Using Reward-Specific and Reward-General Subjective Value Representation in the Brain. J. Neurosci. *31*, 14693–14707.

Levy, D.J., and Glimcher, P.W. (2012). The root of all value: A neural common currency for choice. Curr. Opin. Neurobiol. *22*, 1027–1038.

Liang, F., Paulo, R., Molina, G., Clyde, M.A., and Berger, J.O. (2008). Mixtures of g priors for Bayesian variable selection. J. Am. Stat. Assoc. *103*, 410–423.

Loewenstein, G. (1996). Out of Control: Visceral Influences on Behavior. Organ. Behav. Hum. Decis. Process. *65*, 272–292.

Maris, E., and Oostenveld, R. (2007). Nonparametric statistical testing of EEG- and

MEG-data. J. Neurosci. Methods *164*, 177–190.

De Martino, B., Kumaran, D., Seymour, B., and Dolan, R.J. (2006). Frames, biases and rational decision-making in the human brain. Science (80-.). *313*, 684–687.

McNamara, J.M., Trimmer, P.C., and Houston, A.I. (2012). The ecological rationality of state-dependent valuation. Psychol. Rev. *119*, 114–119.

McNamee, D., Rangel, A., and O'Doherty, J.P. (2013). Category-dependent and category-independent goal-value codes in human ventromedial prefrontal cortex. Nat. Neurosci. *16*, 479–485.

Neubert, F.-X., Mars, R.B., Sallet, J., and Rushworth, M.F.S. (2015). Connectivity reveals relationship of brain areas for reward-guided learning and decision making in human and monkey frontal cortex. Proc. Natl. Acad. Sci. U. S. A. *112*, E2695-704.

Oostenveld, R., Fries, P., Maris, E., and Schoffelen, J.M. (2011). FieldTrip: Open source software for advanced analysis of MEG, EEG, and invasive electrophysiological data. Comput. Intell. Neurosci. *2011*, 1–9.

Padoa-Schioppa, C. (2013). Neuronal origins of choice variability in economic decisions. Neuron *80*, 1322–1336.

Padoa-Schioppa, C., and Assad, J.A. (2006). Neurons in the orbitofrontal cortex encode economic value. Nature *441*, 223–226.

Park, H.-D., and Tallon-baudry, C. (2014). The neural subjective frame: from bodily signals to perceptual consciousness. Philos. Trans. R. Soc. Lond. B. Biol. Sci. *369*, 20130208.

Park, H.-D., Correia, S., Ducorps, A., and Tallon-Baudry, C. (2014). Spontaneous fluctuations in neural responses to heartbeats predict visual detection. Nat. Neurosci. *17*, 612–618.

Peters, E., Joseph, S., Day, S., and Garety, P. (2004). Measuring Delusional Ideation: The 21-Item Peters et aL Delusions Inventory (PDI). Schizophr. Bull. *30*, 1005–1022.

Polanía, R., Krajbich, I., Grueschow, M., and Ruff, C.C. (2014). Neural Oscillations and Synchronization Differentially Support Evidence Accumulation in Perceptual and Value-Based Decision Making. Neuron *82*, 709–720.

Rangel, A. (2013). Regulation of dietary choice by the decision-making circuitry. Nat. Neurosci. *16*, 1717–1724.

Rich, E.L., and Wallis, J.D. (2016). Decoding subjective decisions from orbitofrontal cortex. Nat. Neurosci. *19*.

Ring, C., Brener, J., Knapp, K., and Mailloux, J. (2015). Effects of heartbeat feedback on beliefs about heart rate and heartbeat counting: A cautionary tale about interoceptive awareness. Biol. Psychol. *104*, 193–198.

Schandry, R. (1981). Heartbeat perception and emotional experience. Psychophysiology *18*, 483–488.

Schandry, R., Sparrer, B., and Weitkunat, R. (1986). From the heart to the brain: A study of heartbeat contingent scalp potentials. Int. J. Neurosci. *30*, 261–275.

Sescousse, G., Caldú, X., Segura, B., and Dreher, J.C. (2013). Processing of primary and secondary rewards: A quantitative meta-analysis and review of human functional neuroimaging studies. Neurosci. Biobehav. Rev. *37*, 681–696.

Sherwood, A., Allen, M., Fahrenberg, J., Kelsey, R.M., Lovallo, W.R., and van Doornen, L.J.P. (1990). Methodological Guidelines for Impedance Cardiography. Psychophysiology *27*, 1–23.

Small, D.M., Zatorre, R.J., Dagher, A., Evans, A.C., and Jones-Gotman, M. (2001).

Changes in brain activity related to eating chocolate: From pleasure to aversion. Brain *124*, 1720–1733.

Spielberger, C.D., Gorsuch, R.L., Lushene, R., Vagg, P. R., and Jacobs, G.A. (1983). Manual for the State-Trait Anxiety Inventory. In Consulting Psychologists, (Palo Alto, California), p.

Strait, C.E., Blanchard, T.C., and Hayden, B.Y. (2014). Reward value comparison via mutual inhibition in ventromedial prefrontal cortex. Neuron *82*, 1357–1366.

Tadel, F., Baillet, S., Mosher, J.C., Pantazis, D., and Leahy, R.M. (2011). Brainstorm: A user-friendly application for MEG/EEG analysis. Comput. Intell. Neurosci. *2011*, 879716.

Tzourio-Mazoyer, N., Landeau, B., Papathanassiou, D., Crivello, F., Etard, O., Delcroix, N., Mazoyer, B., and Joliot, M. (2002). Automated anatomical labeling of activations in SPM using a macroscopic anatomical parcellation of the MNI MRI single-subject brain. Neuroimage *15*, 273–289.

Vaidya, A.R., Sefranek, M., and Fellows, L.K. (2017). Ventromedial Frontal Lobe Damage Alters how Specific Attributes are Weighed in Subjective Valuation. Cereb. Cortex *28*, 3857–3867.

Vinck, M., van Wingerden, M., Womelsdorf, T., Fries, P., and Pennartz, C.M.A. (2010). The pairwise phase consistency: A bias-free measure of rhythmic neuronal synchronization. Neuroimage *51*, 112–122.

Zamariola, G., Maurage, P., Luminet, O., and Corneille, O. (2018). Interoceptive accuracy scores from the heartbeat counting task are problematic: Evidence from simple bivariate correlations. Biol. Psychol. *137*, 12–17.